Title

Stimulating the regenerative capacity of the human retina with proneural transcription factors in 3D cultures.

Journal

Proceedings of the National Academy of Sciences, 122(3)

Authors

Wohlschlegel, Juliette

Kierney, Faith

Arakelian, Kayla

et al.

Publication Date

2025-01-21

DOI

10.1073/pnas.2417228122

Peer reviewed

PNAS RESEARCH ARTICLE | NEUROSCIENCE OPEN ACCESS

Stimulating the regenerative capacity of the human retina with proneural transcription factors in 3D cultures

Juliette Wohlschlegel[a], Faith Kierney[a], Kayla L. Arakelian[a], Guillaume Luxardi[b], Naran Suvarnpradip[b], Dawn Hoffer[a], Fred Rieke[c], Ala Moshiri[b], and Thomas A. Reh[a,d,1]

Edited by Jean Bennett, University of Pennsylvania School of Medicine, Bryn Mawr, PA; received August 23, 2024; accepted December 7, 2024

Retinal diseases often lead to degeneration of specific retinal cell types with currently limited therapeutic options to replace the lost neurons. Previous studies have reported that overexpression of *ASCL1* or combinations of proneural factors in Müller glia (MG) induce regeneration of functional neurons in the adult mouse retina. Recently, we applied the same strategy in dissociated cultures of fetal human MG and although we stimulated neurogenesis from MG, our effect in 2D cultures was modest and our analysis of newborn neurons was limited. In this study, we aimed to improve our MG reprogramming strategy in a more intact retinal environment. For this purpose, we used an in vitro culture system of human fetal retinal tissue and adult human postmortem retina. To stimulate reprogramming, we used lentiviral vectors to deliver constructs with a glial-specific promoter (HES1) driving *ASCL1* alone or in combination with additional developmental transcription factors (TFs) such as *ATOH1* and *NEUROD1*. Combining IHC, scRNA-seq, and electrophysiology, we show that human MG can generate new neurons even in adults. This work constitutes a key step toward a future clinical application of this regenerative medicine approach for retinal degenerative disorders.

regeneration | neurogenesis | glia | reprogramming | retina

Significance

The ability to stimulate regeneration of human retinal neurons with a viral gene therapy approach could fundamentally change the way retinal diseases including age-related macular degeneration and glaucoma are treated. Our findings showed that we can stimulate the regenerative capacity of the human retina with viral vectors.

In the mammalian central nervous system (CNS), any loss of neurons, whether accidental, such as through injury, or resulting from the process of aging and disease, is an irreversible process; the retina is no exception to the rule. Retinal degeneration is one of the leading causes of blindness, and retinal diseases like age-related macular degeneration impose a great personal as well as an economic burden worldwide. While new therapeutic strategies and technologies are constantly emerging to delay the progression of retinal diseases, restoration of visual function after cellular degeneration has occurred is still not possible. In the field of regenerative medicine, cell transplant and regeneration are two complementary approaches used to replace the damaged cells and ultimately restore visual function (1–3). Regenerative strategies offer the advantage of utilizing endogenous cells, thereby eliminating some of the complexities of cell transplantation, including abrogating the need for immunosuppressant therapies.

Several studies in the last few years demonstrated that Müller glia (MG), the principal retinal glial cells, can be reprogrammed to generate neurons in the adult mouse retina (4–10). Inspired by the regenerative capacity of nonmammalian vertebrate retina (11–13), this strategy relies on overexpressing the proneuronal transcription factor (TF) *Ascl1* in MG (5, 6, 14). With this strategy, newly generated neurons are integrated into the existing circuit, and molecularly and functionally resemble inner retinal neurons, primarily bipolar cells (4–6). Additional studies have made significant progress boosting the efficiency of MG reprogramming and expanding the cell fate diversity of MG-derived neurons in the mouse retina (8, 15–17). For instance, the combination of the developmental TFs *Islet1* and *Pou4f2*, along with *Ascl1* can reprogram MG into RGC-like cells (7). This work supports the feasibility of restoring retinal cell types in the adult mammalian retina; however, these studies relied on Cre-dependent transgenic mouse models, which cannot be directly translated to humans.

In a recent study, we demonstrated that dissociated cultures of human fetal or organoid-derived MG can be reprogrammed into neurons using a lentivirus expressing *ASCL1* (18). Consistent with previous studies in mice, most of the MG expressing *ASCL1* are converted to neurogenic precursors and only a subpopulation generated neurons (18). Interestingly, human MG-derived neurons resemble immature amacrine-like, and RGC-like cells, as opposed to mouse MG–derived neurons that more closely resembled bipolar cells. Although, these results present a proof of principle that

Author affiliations: [a]Department of Biological Structure, University of Washington, Seattle, WA 98125; [b]Department of Ophthalmology & Vision Science, University of California Davis School of Medicine, Sacramento, CA 95616; [c]Department of Physiology and Biophysics, University of Washington, Seattle, WA 98125; and [d]Institute for Stem Cells and Regenerative Medicine, University of Washington, Seattle, WA 98125

Author contributions: J.W. and T.A.R. designed research; J.W., F.K., K.L.A., G.L., N.S., D.H., F.R., and A.M. performed research; J.W., F.R., and A.M. contributed new reagents/analytic tools; J.W., F.R., and T.A.R. analyzed data; and J.W., F.R., and T.A.R. wrote the paper.

Competing interest statement: Some of the research described is included in a patent owned by the University of Washington and licensed to Tenpoint Biopharma. T.A.R. has equity in Tenpoint. U.S. Patent Application Serial No. 17/050,999 filed October 27, 2020 for methods and compositions to stimulate retinal regeneration. T.A.R. receives consulting fees from Tenpoint Biopharma.

This article is a PNAS Direct Submission.

[1]To whom correspondence may be addressed. Email: tomreh@uw.edu.

This article contains supporting information online at https://www.pnas.org/lookup/suppl/doi:10.1073/pnas.2417228122/-/DCSupplemental.

Published January 17, 2025.

human MG can also be reprogrammed into neurons, those neurons do not fully differentiate in dissociated cultures, likely due to a lack of environmental cues.

In this study, we aimed to reprogram human MG in a more intact and physiologically relevant retinal environment. For this purpose, we used explant cultures of fetal and adult postmortem retinal tissue. We further designed a lentiviral strategy that uses the *HES1* promoter (19, 20) to precisely drive expression of reprogramming TFs in MG, to stimulate neurogenesis in these cells. One major advantage of this approach is the maintenance of the expression of *ASCL1*, even as cells reprogrammed from glia to progenitor cells, since *HES1* is also expressed in progenitor cells during fetal development. Using this approach, we now demonstrate that neural regeneration can be stimulated in both fetal and adult human retinas. This work provides a crucial step toward translation of in vivo reprogramming as a therapy for retinal diseases.

Results

HES1 Promoter in a Lentiviral Construct Drives Expression Specifically in Human MG (Fig. 1 and *SI Appendix*, Fig. S1). To identify potential promoters that could be used for stimulating reprogramming in MG, we examined Multiome data from a D59 human fetal retina and selected promoters that are accessible in both MG and retinal progenitors (18). Our rationale was that these promoters would potentially be active both in the target glial population and the glial-derived progenitors as they are reprogrammed. We identified *HES1* as an ideal candidate, since this gene is expressed both in MG and in progenitors in the snRNA-seq data (Fig. 1 *A*, *Right*) and the snATAC-seq results show accessibility in both cell types in the region corresponding to the human HES1 promoter (Fig. 1 *A*, *Left*). After confirming the expression of HES1 in human MG (*SI Appendix*, Fig. S1*A*), we then designed and generated lentiviral constructs with the HES1 promoter driving the expression of *ASCL1* followed by a fluorescent protein (GFP). We also generated a control vector, with HES1 promoter driving GFP.

We generated retinospheres from fetal retinal tissues of different gestational ages as previously described (18). Retinospheres were maintained in vitro culture for various lengths of time. In the human retina, MG arise around fetal week 8 in the central retina and later in other regions, following a central to peripheral gradient. For the rest of the study, we used retinospheres that were older than 200 d; however, one sample was 174 d, but this was taken from the central retina, where our previous study showed that MG are already well developed by that time (18). Retinospheres from different samples and at different ages were infected with the constructs (HES1-GFP and HES1-ASCL1-GFP). To ensure reproducibility, each retinosphere from the same condition was infected individually and received the same cocktail of virus (18).

Retinospheres were infected with the HES1-GFP or HES1-ASCL1-GFP viral vectors, fixed at different time points [7-, 14-, and 20-d post infection (dpi)] (Fig. 1*B*) and later sectioned and immunolabeled with different neuronal and glial markers (Fig. 1 *D* and *E*). By 4 dpi, GFP was already detectable in both conditions (Fig. 1*C*). To test the glial specificity of the HES1 promoter, we then focused on the HES1-GFP condition. At 7 dpi, immunohistochemistry (IHC) analysis revealed that GFP+ cells colocalized with the HES1 glial marker (Fig. 1*D*) and that the cell type specificity was maintained at 14- and 20-dpi (Fig. 1*D*). Furthermore, at 20 dpi, GFP+ cells expressed the SOX9 glial marker and did not express OTX2 or HuC/D, two neuronal markers (Fig. 1*E*). Quantification of the GFP+ cells further validated this result showing that the number of GFP/OTX2+ neurons was minimal and constant over time (6 retinospheres per time point, average of 1.33% at 7-, 14-, and 20-dpi) (Fig. 1*F*). These results demonstrated the HES1 promoter exhibits a glial-restricted activity in retinospheres.

Efficient Reprogramming of Human MG in 3D Retinospheres with the HES1-ASCL1-GFP Viral Vector (Fig. 2 and *SI Appendix*, Figs. S2 and S3). To detect the expression of ASCL1, sections were immunolabeled with a MASH1 (ASCL1) antibody at 7 dpi and 14 dpi. In the HES1-ASCL1 infected condition, we observed a robust expression of ASCL1 that was absent in the control condition (HES1-GFP) (*SI Appendix*, Fig. S2*A*). Similarly, cells infected with the HES1-ASCL1 construct still express ASCL1 14 dpi (*SI Appendix*, Fig. S2*B*). To determine whether the expression of a proneural TF would change the glial specificity of the HES1 promoter, a phenomenon that has confounded previous studies on reprogramming glia into neurons (21–23), retinospheres were infected with the ASCL1 construct and fixed at 2 dpi, when the first GFP+ cells were detectable. We reasoned that 2 d would not be sufficient time for MG to be reprogramed to neurons, so any GFP expression in neurons would indicate a change in the glial specificity of the HES1 promoter. We found that after 2 dpi, GFP+ cells were primarily colabeled with SOX9, and did not express the OTX2 neuronal marker (%SOX9 + GFP+/GFP+, 97.6%) (*SI Appendix*, Fig. S2*C*). Furthermore, we found ASCL1 expression in SOX9/GFP+ cells (*SI Appendix*, Fig. S2*D*). We therefore conclude that during the first two days following the infection, the addition of the *ASCL1* to the lentiviral construct did not modify the specificity of the promoter: We saw no evidence of GFP expression in neurons.

To determine whether longer expression of the proneural TF would induce neurogenesis in the MG, we infected retinospheres as above and then incubated them for 7 or 14 d (Fig. 2*A*). In addition, EdU (5-ethynyl-2'-deoxyuridine) was continuously added to the medium to track the generation of new cells. We found that in the HES1-ASCL1-GFP condition, GFP+ cells acquired a more pronounced neuronal morphology, with a smaller and rounder nucleus, and tended to migrate to the outer nuclear layer (ONL) (Fig. 2*B*). While GFP+ cells from the control condition were all positive for the MG marker SOX9 and negative for the neuronal marker OTX2, 22% and 24% of the GFP+ MG-derived cells from the 7 and 14 dpi treatment groups, respectively, expressed OTX2 (Fig. 2*C*). Other neuronal markers such as HuC/D (expressed by RGCs and amacrine cells) were also tested; however, we observed a very low number of GFP/HuC/D+ cells (*SI Appendix*, Fig. S2 *F* and *E*, 2,5% across five retinospheres from two donors). Of note, we noticed a decrease in reprogramming efficiency over time as the retinospheres age: Approximately 35% of the GFP+ cells generated OTX2+ neurons from retinospheres infected at D209, whereas this number was decreased to only 21% at D300-D313 (Fig. 2*D*).

We then calculated the percentage of infected cells that were EdU+ and found that almost half of the GFP+ cells were EdU+ (43.5% of %EdU+GFP+/GFP+) (Fig. 2 *E* and *F*). This was particularly visible for the younger retinospheres compared to the older ones (Fig. 2*F*). To determine whether new OTX2+ neurons resulted from trans-differentiation or MG proliferation, we quantified the number of GFP/OTX2+ cells colabeled with EdU (Fig. 2*G*). Interestingly, most of the EdU+ infected cells did not express OTX2, (%OTX2+/EdU+GFP+, 18.6% in the ASCL1 condition, Fig. 2*G*) showing that most of the infected MG directly trans-differentiated into neurons without reentering the cell cycle (Fig. 2*H*).

Our success with using the HES1 promoter to stimulate neurogenesis from MG in human 3D cultures, suggests that this promoter could be a more general strategy for neural reprogramming in mice as well. To test whether the HES1 promoter can also drive

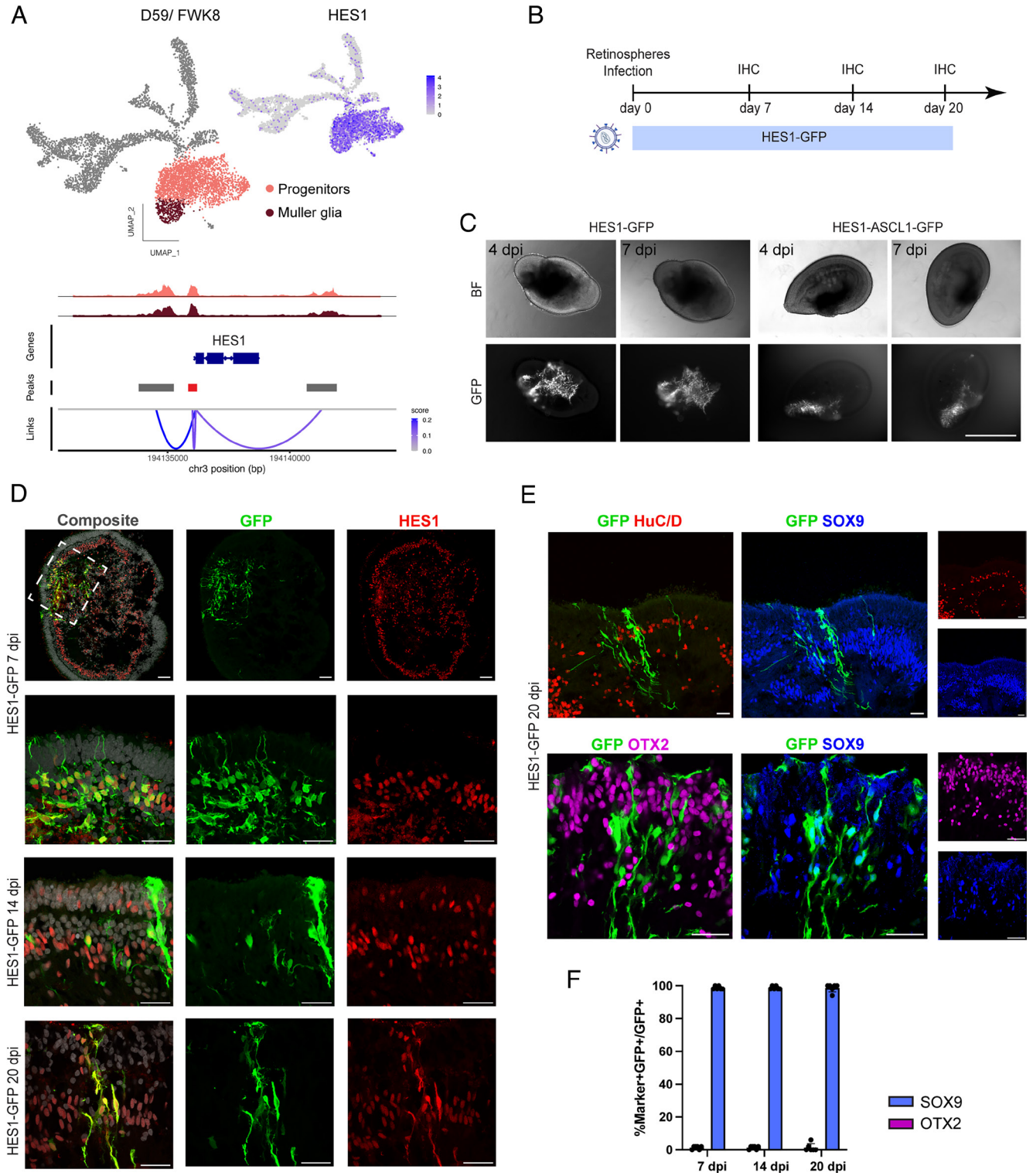

Fig. 1. HES1 promoter displays a glial-restricted activity in retinospheres. (*A*) Multiome data from a D59 fetal human retinal sample. *Top Left* UMAP plot from snRNA-seq data organized by cell type [orange; retinal progenitors and dark red: Muller glia (MG)]. *Top Right*: Feature plot showing HES1 expression in the progenitor and MG clusters. *Bottom*: coverage plot nearby *HES1* showing peak to gene analysis, data obtained from the snATAC-seq data. The red sequence represents the presumed sequence of the HES1 promoter. (*B*) Schematic of the experimental timeline to test the specificity of the HES1 promoter. (*C*) Retinospheres infected with the different lentiviral constructs at 4- and 7-d post infection. *Top* panels show the brightfield (BF) images and *Lower* panels show the GFP reporter expression. (Scale bar, 500 μm.) (*D*) HES1 expression colocalized with GFP+ cells at 7-, 14-, and 20 d post infection with the HES1-GFP virus. DAPI (gray), GFP (green), and HES1 (red). [Scale bar, 50 μm (*Top* row); Scale bar, 30 μm (*Lower* panels).] (*E*) Representative images showing that GFP+ cells do not colocalized with the HuC/D (red) nor OTX2 (magenta) neural markers 20 d post infection (dpi) with the HES1-GFP virus. (Scale bar, 30 μm.) (*F*) Quantification showing a residual number of GFP/OTX2+ cells after HES1-GFP infection, [6 retinospheres per timepoint, 7 dpi (2 × D245, 4 × D343), 14 dpi (2 × D209, 4 × D255), 20 dpi (1 × D209, 2 × D255, 2 × D301)].

reprogramming in mouse MG, retinas from P12 and adult mice were cultured as explants and infected with the same lentiviral constructs used for the human (*SI Appendix*, Fig. S3*A*). At 7 dpi, retinal explants were fixed and immunolabeled with the same markers used for the retinospheres. In absence of ASCL1, GFP+ cells expressed the glial markers HES1 and SOX2, validating the

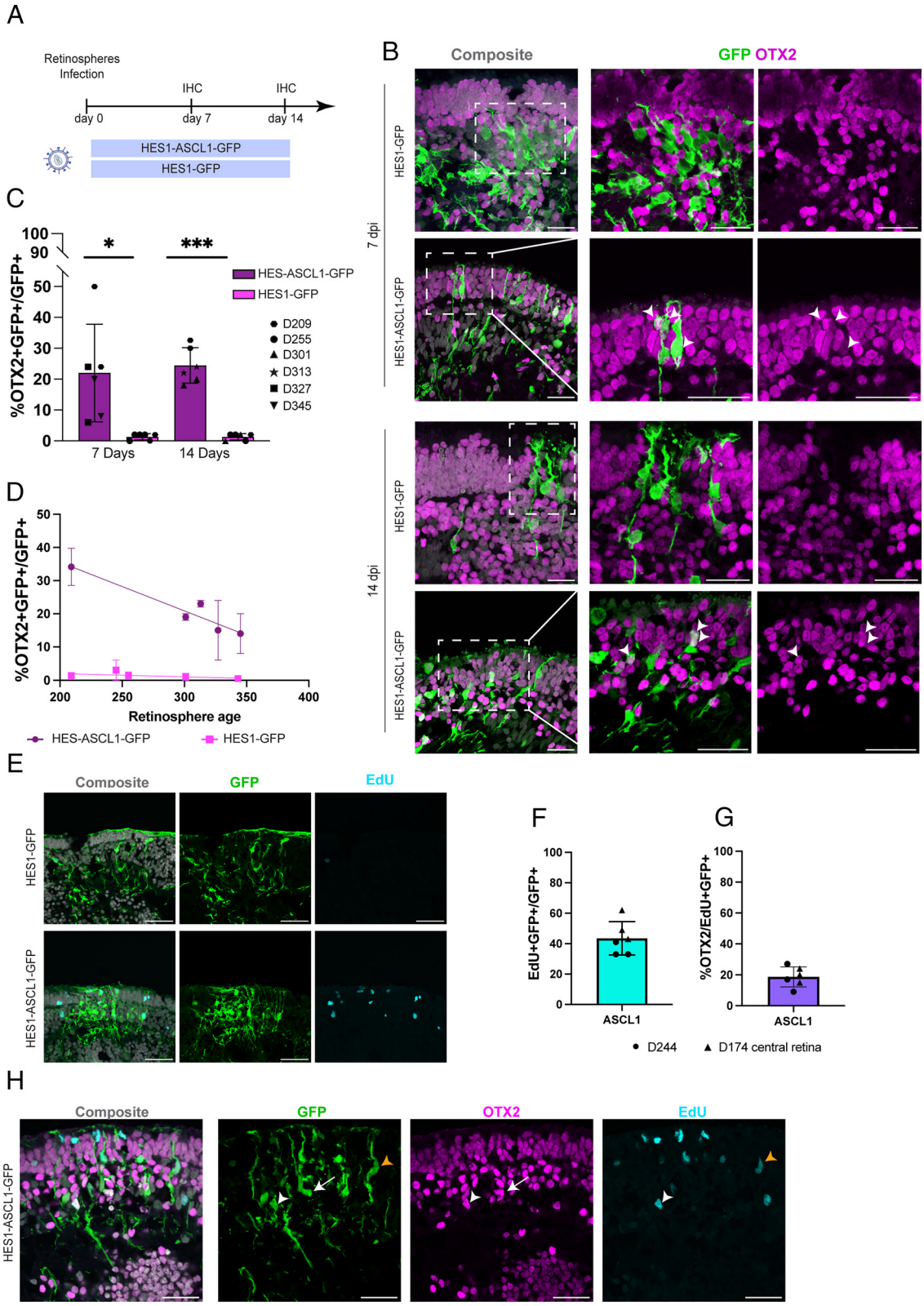

Fig. 2. Expression of ASCL1 via the HES1 promoter enables MG reprogramming into neurons in retinospheres. (*A*) Schematic of the workflow to test MG reprograming with the HES1-ASCL1-GFP lentivirus. (*B*) Representative images showing MG-derived neurons expressing OTX2 (magenta) after ASCL1 expression at 7- and 14-d post infection. Arrowheads show colabeled GFP/OTX2+ cells. DAPI (gray). (On the *Left* side of the panel, Scale bar, 25 μm and Scale bar, 30 μm on the *Right* side of the panel.) (*C*) Quantification of the percent of GFP+ MG-derived neurons that express OTX2, 7- and 14-d post infection. Each shape represents a retinosphere. Ages of the retinospheres are indicated on the *Right* side of the figure. Significance was determined by a Welch's *t* test (*$P < 0.05$, ***$P < 0.001$). (*D*) Reprogramming efficiency decreases with the ages of the retinospheres. Each shape (purple dots for HES1-ASCL1 and pink squares for HES1-GFP) represents all the combined data for this specific age. Data are represented as mean ± SEM. (*E*) Representative images showing MG proliferation after ASCL1 overexpression and in the control condition (HES1-GFP), GFP (green), EdU (cyan), and DAPI (gray). (Scale bar, 50 μm.) (*F*) Quantification of GFP+ cells colabeled with EdU after ASCL1 overexpression. (*G*) Quantification of MG-derived newborn OTX2+ cells after ASCL1 overexpression. Each shape represents a retinospheres. (*H*) Confocal images showing MG to neurons conversion. White arrows show GFP/OTX2+ cells, orange arrowheads indicate GFP/EdU+ cells, and white arrowheads show GFP/OTX2/EDU+ cells. (Scale bar, 30 μm.)

specificity of the HES1 promoter for mouse MG (*SI Appendix*, Fig. S3*B*). In the HES1-ASCL1 condition, most GFP+ cells acquired a neuronal morphology and expressed MASH1(ASCL1) and OTX2 (*SI Appendix*, Fig. S3*C*). After ASCL1 expression, we found a similar fraction of GFP/OTX2+ cells as previously observed in human retinospheres (27%) (*SI Appendix*, Fig. S3*D*). In the ASCL1-infected MG, we found some GFP/OTX2+ cells also labeled with EdU demonstrating that they were newborn neurons (*SI Appendix*, Fig. S3*E*). In addition to the P12 mouse retinal explants, we also tested the ASCL1 virus on adult mouse retinal explants; however, we did not detect any GFP/OTX2+ neurons (*SI Appendix*, Fig. S3 *F* and *G*). This result is consistent with previous studies demonstrating transgenic expression of ASCL1 alone is not sufficient to stimulate the MG neurogenesis in the adult mouse retina (5, 6, 24).

Lentiviral-Mediated Combinations of bHLH Increase MG to Neuron Reprogramming Efficiency (Fig. 3 and *SI Appendix*, Fig. S4). Previous studies in mice demonstrated that additional TFs along with ASCL1 influence the cell fate of MG-derived neurons (7, 8). To test this strategy in human 3D cultures, we designed an additional lentiviral construct containing ASCL1-ATOH1-GFP under the HES1 promoter. The new construct was first tested on retinospheres, following the same paradigm as previously described (Fig. 3*A*).

We then performed IHC with several neuronal markers. Most of GFP+ cells acquired a neuronal morphology, and we found many GFP+ cells colocalizing with OTX2 or HuC/D (Fig. 3*B*). As OTX2 and HuC/D are markers of distinct populations of neurons (i.e., photoreceptors/bipolar cells and RGCs/amacrine cells, respectively), the results showed that expressing this combination of TFs (ASCL1 and ATOH1) can expand the diversity of neuronal types generated from MG in humans, much like what this combination does in mice (8). In addition, ASCL1-ATOH1 infected cells demonstrated a global increase in reprogramming efficiency compared to ASCL1 alone, similar to our observations in transgenic mice. Interestingly, in human retinospheres, coexpression of ASCL1 and ATOH1 leads to a higher proportion of MG-derived neurons expressing the OTX2 marker compared to HuC/D (53.6% for OTX2 and 11.5% for HuC/D) (Fig. 3*C*). This is different from mice, where the majority of MG-derived neurons expressed HuC/D and acquired an immature RGC phenotype (8).

To determine whether this difference between human and mouse MG is maintained using the lentiviral construct, P12 (*SI Appendix*, Fig. S4 *A* and *B*) and adult mouse (*SI Appendix*, Fig. S4 *C* and *D*) retinal explants were then infected with the ASCL1-ATOH1 virus. IHC analysis on P12 explants sections (*SI Appendix*, Fig. S4*B*) and wholemount (*SI Appendix*, Fig. S4*D*) revealed that most GFP+ cells express HuC/D after infection with both ASCL1 and ATOH1 showing that mouse and human MG can respond differently to the same TFs.

As already mentioned, studies in mice demonstrated that combinations of developmentally expressed TFs could affect the reprogramming process (7). We next tested whether combining another developmental proneural TF, NEUROD1, along with ASCL1 would enhance MG neurogenesis. We infected retinospheres with HES1-NEUROD1-ASCL1-GFP, HES1-ASCL1-GFP, or HES1-GFP lentiviruses (Fig. 3*D*). In the NEUROD1 condition, we observed more GFP+ cells expressing the neuronal marker OTX2 compared to the control condition (60% for NEUROD1-ASCL1 versus 27% for ASCL1 alone) (Fig. 3 *E* and *F*). In addition, we did not observe any GFP/HuC/D+ neurons in the NEUROD1 condition.

Since the combination of ASCL1 and NEUROD1 was particularly effective at stimulating neurogenesis in MG from the human retina, we also tested this construct on adult mouse retinal explants (*SI Appendix*, Fig. S4*E*). One week post infection, IHC analysis revealed some GFP+ cells that expressed the OTX2 neuronal marker (*SI Appendix*, Fig. S4*F*). Interestingly, the SOX9 glial marker was still expressed in many reprogrammed MG (*SI Appendix*, Fig. S4*F*).

Overall, these results demonstrate that combining different TFs along with ASCL1 increased the efficiency of MG reprogramming.

Combination of ASCL1 and NEUROD1 Induces More Bipolar-Like Cells Compared to ASCL1 Alone (Fig. 4 and *SI Appendix*, Fig. S5). Since both ASCL1 only and NEUROD1-ASCL1 viruses produce MG-derived OTX2+ neurons, we next conducted single-cell RNAseq (sc-RNAseq) to better analyze how these two conditions differed. For this, we infected retinospheres at D203 with HES1-NEUROD1-ASCL1-GFP, HES1-ASCL1-GFP, and HES1-GFP (Fig. 4*A*). At 14 dpi, retinospheres were dissociated and the GFP+ cells were isolated using fluorescence-activated cell sorting (FACS) prior processing for scRNA-seq. For all conditions, the GFP+ cell fractions were extracted and processed as individual samples. Datasets were then merged on a single UMAP (uniform manifold approximation and projection) plot (*SI Appendix*, Fig. S5*A*) containing different cell clusters that were identified based on the expression of well-known marker genes (*SI Appendix*, Fig. S5*B*). As expected, we found a cluster of MG and a cluster of astrocytes that both express HES1. We also noticed additional cell clusters of cones, rods, and amacrine cells, which are present in all samples, and we assume are carried over from the cell sorting (*SI Appendix*, Fig. S5 *A* and *B*). We further subset the MG and MG-derived cell clusters for further analysis (Fig. 4*B*). The subset merged UMAP plot contains cell clusters of the following: 1) MG; 2) Proliferating MG; 3) Neurogenic precursors; 4) Bipolar cell precursors; 5) Bipolar cells and 6) Nonidentified cells (NDC) (Fig. 4 *B* and *C*).

Our results confirm the IHC results described above (Fig. 3*E*) that ASCL1 and NEUROD1-ASCL1 conditions stimulate the neurogenic capacity of the MG. We found that infection with ASCL1 causes a decrease in expression of *RLBP1* and *HES1* and an increase in expression of neurogenic precursors genes, such as *HES6* (Fig. 4*D*). Furthermore, the addition of NEUROD1 further promotes neurogenic capacity of the MG, since we observed more cells present in the Bipolar cell cluster in this condition compared to ASCL1 alone (Fig. 4 *D* and *E*).

We detected the expression of both OTX2 and PCP2 in the MG-derived neurons (neurogenic precursors, bipolar cell precursors, and bipolar cells) (Fig. 4*D*). PCP2 is a well-known marker of ON bipolar cell in the mouse retina (25, 26). We confirmed the ON-bipolar restricted expression of PCP2 in the fetal human retina using IHC on a D150 retinal section and found PCP2+ cells located in the INL and colocalized with OTX2 (*SI Appendix*, Fig. S4*C*). Next, we used the same PCP2 antibody and confirmed that the protein is expressed in MG-derived neurons in both ASCL1 and NEUROD1-ASCL1 conditions. Interestingly, we were able to detect PCP2 at 7 dpi in the NEUROD1-ASCL1 condition, but only later, at 14 dpi in the ASCL1 condition (Fig. 4*F*).

Since HES1 is also expressed in progenitors, we noticed some residual neurogenesis in the control condition (CTL: HES1-GFP), even without the expression of TFs; this is likely due to the presence of a small pool of progenitors (Fig. 4*C*). To ensure that our results are due to MG reprogramming and not normal developmental neurogenesis, we performed an additional experiment where retinospheres were treated with a notch inhibitor for three days prior to infecting with the viral constructs (*SI Appendix*, Fig. S5*D*); inhibition of notch signaling will force all remaining progenitors to differentiate (27–30). After infection with ASCL1 in the retinospheres

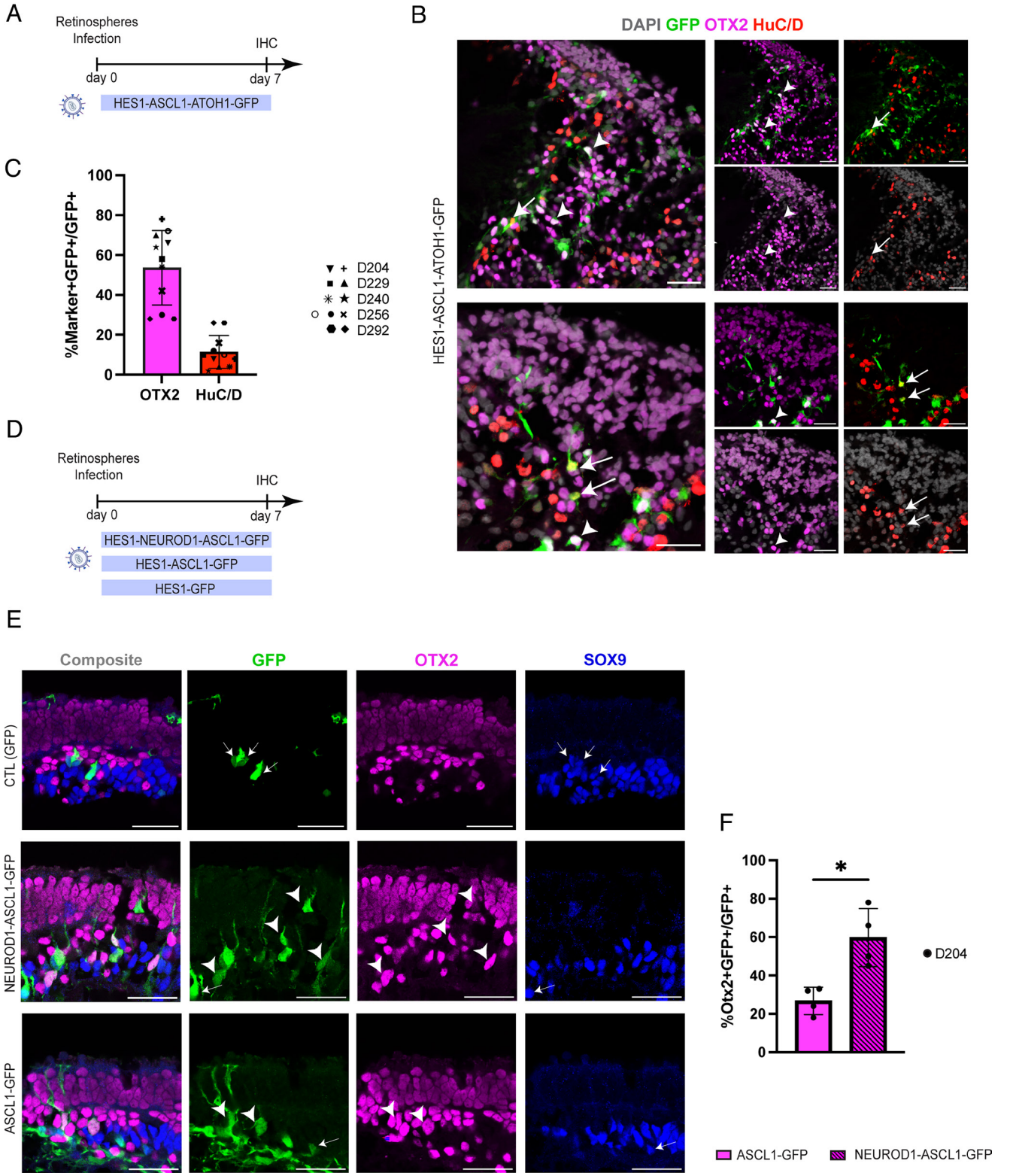

Fig. 3. Combinations of TFs enhance MG reprogramming efficiency in retinospheres. (*A*) Schematic of the experimental workflow to test MG reprograming with the HES1-ASCL1-ATOH1-GFP lentivirus. (*B*) Representative images showing MG-derived neurons expressing OTX2 (magenta) or HuC/D (red) after ASCL1-ATOH1 expression at 7 dpi. Arrowheads show colabeled GFP/OTX2+ and arrows indicate GFP/HuC/D+ cells. DAPI (gray). (Scale bar, 30 μm.) (*C*) Quantification of the MG-derived neurons expressing OTX2 or HuC/D. Each shape represents a retinosphere and ages of the retinospheres are indicated on the *Right* side of the figure. (*D*) Schematic of the experimental workflow used to test HES1-NEUROD1-ASCL1-GFP. (*E*) Representative images showing MG-derived neurons expressing OTX2 (magenta) and not SOX9 (blue) 7 d after ASCL1 or NEUROD1-ASCL1 overexpression. Arrowheads show colabeled GFP/OTX2+ cells. Arrows show GFP/SOX9+ cells. DAPI (gray). (Scale bar, 30 μm.) (*F*) Quantification of the MG-derived neurons expressing OTX2. Each dot represents a retinosphere. [8 × D204]. Significance was determined by a Welch's *t* test (*$P < 0.05$).

treated with the notch inhibitor, we found that ASCL1 induced MG-derived OTX2+ cells (15.4%) as well as in the retinospheres that did not receive the notch inhibitor (*SI Appendix*, Fig. S5 *E* and *F*). Therefore, it is likely that the new neurons we observe in ASCL1-infected retinospheres are arising from MG, not residual progenitors.

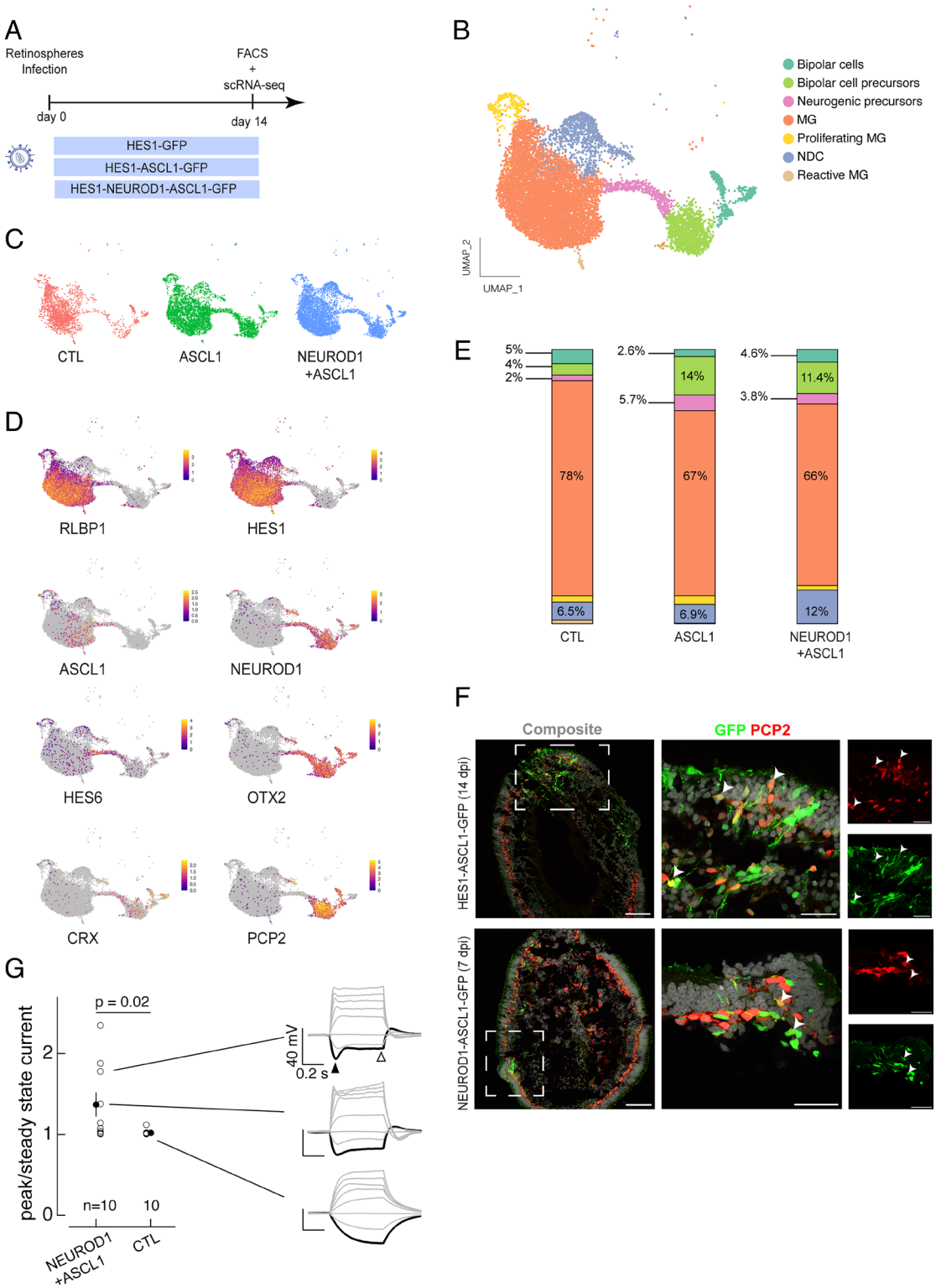

Fig. 4. Addition of NEUROD1 along ASCL1 enhances MG reprograming efficiency and promotes functional newborn neurons. (*A*) Schematic of the experimental workflow. (*B*) Merged UMAP plot of the three conditions (HES1-GFP, HES1-ASCL1, and HES1-NEUROD1-ASCL1). (*C*) Merged UMAP plot split by conditions showing the distribution of the different clusters for each condition. (*D*) Feature plots showing the expression of different genes (*RLBP1*, *HES1*, *ASCL1*, *NEUROD1*, *HES6*, *OTX2*, *CRX,* and *PCP2*). (*E*) Stacked bar plots indicating the percentages of each cell type cluster per condition. (*F*) Retinospheres sections labeled with PCP2 (red) and GFP (green), DAPI (gray). Arrowheads show colabeled GFP/PCP2+ cells. (Scale bar, 100 μm and Scale bar, 30 μm in higher magnification.) (*G*) Summary of electrical properties of reprogrammed cells in the NEUROD1-ASCL1 condition 10 dpi. *Right* three panels show voltage responses to a family of current steps from two reprogrammed cells (*Top* two panels) and one control transfected cell (HES1-GFP) (*Bottom*). The *Center* panel measures the rebound in voltage in response to a hyperpolarizing current step using the ratio of the peak to steady state voltage change (e.g., ratio of voltage changes at the times of the closed and open arrowheads in the *Top Right* panel).

Last, we focused on the NEUROD1-ASCL1 condition to test the electrical properties of the MG-derived neurons by performing whole-cell patch clamp recordings from GFP+ cells in retinospheres (Fig. 4*G*). We were particularly interested in whether the complement of ion channels expressed by the cells was affected by TF reprogramming, resulting in changes in the voltage responses to

injected current. To test ion channel expression, we measured voltage responses to a family of injected currents (Fig. 4*G*). Some of the reprogrammed cells showed a clear rebound in voltage following a hyperpolarizing current step (e.g., black trace in *Upper Right* panel of Fig. 4*G*). A hyperpolarization-activated current produces similar voltage rebounds in many neurons, including several retinal neuron types. In addition, voltage-clamp recordings revealed a slowly activating inward current following a hyperpolarizing voltage step (*SI Appendix*, Fig. S5*G*). We quantified the rebound in voltage by measuring the ratio of the peak voltage change (filled arrowhead in *Top Right* panel of Fig. 4*G*) to the steady-state voltage change (open arrowhead). Fig. 4*G* plots these ratios for each reprogrammed cell and each matched control cell. Four of ten reprogrammed cells and none of 10 control cells showed such a rebound; on average, the difference in peak vs steady-state ratio was significantly larger in reprogrammed cells compared to matched controls (HES1-GFP). Overall, this result demonstrated that MG-derived cells induced by NEUROD1-ASCL1 display electrophysiological properties different from typical glial cells and more comparable to neurons.

Together our results demonstrated that in both conditions, ASCL1 and NEUROD1-ASCL1, induced MG-derived neurons that resemble bipolar cells. Furthermore, the combination of NEUROD1-ASCL1 stimulates neurogenesis in MG with a higher efficiency than ASCL1 alone.

MG Reprogramming in the Human Adult Postmortem Retina (Fig. 5). The results with the fetal retinospheres demonstrated that human MG can be reprogrammed to neural progenitors to regenerate retinal neurons; however, it is not known whether adult human MG can be reprogrammed to neural progenitors. This is a critical next step to evaluate the feasibility of in vivo reprogramming for regenerative medicine. To determine whether neurogenesis can be stimulated in adult human MG, we used human adult postmortem retinas, cultured as explants. Previous studies have shown that forced expression of ASCL1 alone in mature mouse MG is no longer sufficient to induce MG reprogramming (5, 6). However, the combination of ATOH1 along with ASCL1 has proven to be efficient in reprogramming adult MG in the mouse retina (7, 8). Therefore, we tested several combinations of reprogramming factors in adult human postmortem retinas.

Retinal explants were initially infected with HES1-GFP or HES1-ASCL1-GFP lentivirus and fixed 7 dpi prior to immunolabeling with different glial and neuronal markers (Fig. 5*A*). We observed a widespread lentiviral infection on human postmortem explants (Fig. 5*B*). We first confirmed the specificity of the HES1 promoter; all GFP+ expressing cells were colabeled with the SOX9 glial marker (%SOX9+GFP+/GFP+, 100%). In the control condition, cells retained a MG morphology, with processes spanning the entire retina (Fig. 5*C*). Of note, some explants also contained some GFP/SOX9+ cells in the ganglion cell layer (GCL), showing that astrocytes were also infected. In the ASCL1 condition, despite ASCL1 expression (GFP/MASH1+ cells), GFP+ cells still retained a MG morphology and did not express OTX2 (Fig. 5*C*). Therefore, ASCL1 alone was not sufficient to stimulate neurogenesis from adult human MG, though it had this potential in the fetal MG.

Results from mice demonstrated that the combination of ASCL1 and ATOH1 was much more efficient in stimulating neurogenesis in adult MG. Therefore, we next infected adult postmortem retinal explants with a virus expressing both ASCL1 and ATOH1, following the same paradigm as described above. Due to the size of the polycistronic transgene cassette, where the fluorescent reporter is on the third position, we detected fewer GFP+ cells in this condition. However, some GFP+ cells exhibited a neuronal-like morphology, with a rounder and smaller nucleus, contrasting with the two previous conditions (HES1-GFP and HES1-ASCL1-GFP). Further IHC analysis showed some GFP+ cells expressed OTX2 (Fig. 5*D*). In rare case, we also found some GFP/HuC/D+ cells (Fig. 5*D*). In both cases, the glial/progenitor marker HES1 was still detectable in the MG-derived neurons and not observed in other conditions (HES1-GFP and HES1-ASCL1). Similarly, we also found some GFP/OTX2/MASH1+ cells in the HES1-NEUROD1-ASCL1 condition (Fig. 5*E*). Therefore, the labeling of HES1 or MASH1 (ASCL1) with neuronal markers such as OTX2 and HuC/D further validated that neurons are derived from MG, since this labeling was not present in the control. Taken together, our results demonstrate that MG can be reprogrammed into neurons in the adult human retina using a combination of proneural bHLH TFs.

Discussion

In the last ten years, studies in mice, and more recently humans, have shown that MG can be stimulated to generate neurons (6–9, 18, 31). In this study, we aimed to determine whether this same approach can be used in the human retina: Can human MG be reprogrammed to a neurogenic state? These studies are of necessity in vitro, and so we employed explant cultures of both adult human postmortem retina and human fetal retina (18, 32, 33). We identified a promoter from the HES1 gene that is active in both glia and progenitor cells, to drive the expression of proneural factors including ASCL1, ATOH1, and NEUROD1. The HES1 promoter has the unique advantage of showing glial specificity to initiate the reprogramming process, and expression in the glial-derived progenitor cells, thus providing an approach to design of reprogramming strategies. We used this design to show that human MG can be stimulated to generate neurons in both adult and fetal retinas. This provides a proof of concept that in vivo reprogramming to stimulate neurogenesis from glia can provide an approach for repairing the CNS. The expression of the proneural TF *Ascl1* can stimulate neurogenesis from MG in mice, and now we demonstrate that this is possible in human glia as well: MG-specific expression of *ASCL1* alone in the retinosphere MG produces OTX2+ neurons. Although the MG reprogramming efficiency can be greater than 20% in retinospheres with ASCL1, we noticed a decrease in MG neurogenesis with the age of the retinospheres and there were no MG-derived neurons in the adult retina after ASCL1 overexpression alone. In younger retinospheres, the higher reprogramming efficiency could partially be explained by the presence of residual progenitors (or less mature MG), particularly in retinospheres from the most peripheral regions of the retina. Furthermore, we observed a low level of neurogenesis in the GFP control condition in our scRNA-seq data. In future studies, it will be important to understand the role of glial maturation in their ability to become neurogenic. In addition, keeping track of the different retinal regions from which retinospheres are generated will be important as this could highlight potential differences in reprograming efficiency. Nonetheless, the difference in reprogramming efficiency between fetal and adult human MG mirrors that observed in mice, with a progressive loss of the MG neurogenic capacity over time due to epigenetic changes (6, 24). In the adult mouse retina, this issue has been overcome using Trichostatin A (TSA), an epigenetic modulator, along with expression of ASCL1 (6–8). Although the expression of ASCL1 alone was not sufficient to stimulate neurogenesis in adult human MG, we have previously shown that combinations of proneural TFs can substantially increase the efficiency of the reprogramming process in mice. Therefore, we also tested combinations of proneural TFs in the human retinal explants and found that combining ASCL1 with either ATOH1 or NEUROD1, significantly increases the efficiency of neurogenesis in fetal MG. The combination

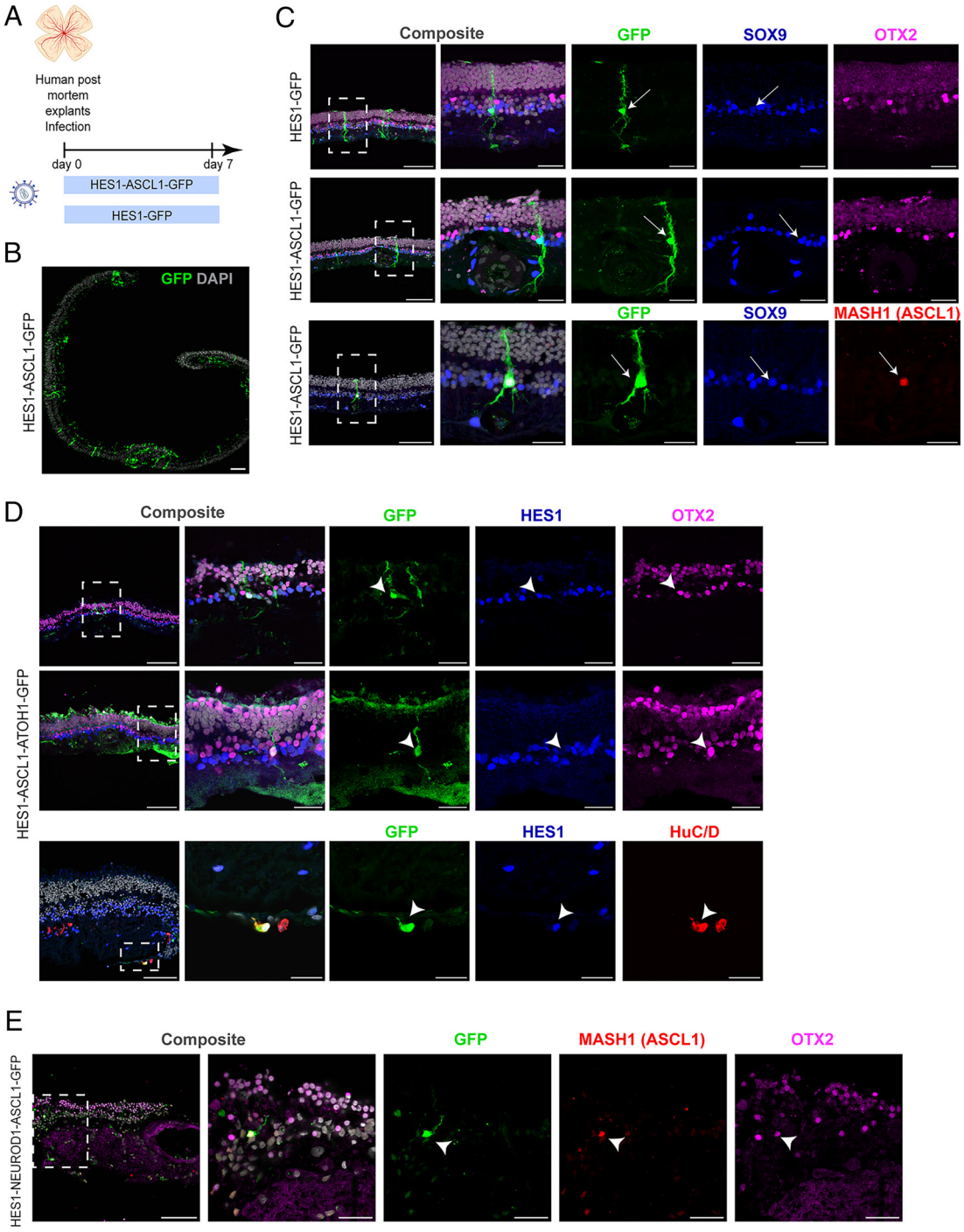

Fig. 5. MG reprogramming in the adult human retina in vitro. (*A*) Schematic of the experimental workflow to test MG reprograming in adult postmortem retinal explants. (*B*) Representative images showing the infection efficiency with the HES1-ASCL1 lentivirus in the adult postmortem retinal explants. DAPI (gray) and GFP (green). (Scale bar, 100 μm.) (*C*) Representative images showing that HES1 drives the expression of ASCL1 (MASH1, red), but it is not sufficient to reprogram human adult MG in vitro. SOX9 (blue), GFP (green), OTX2 (magenta), MASH1 (ASCL1, red), and DAPI (gray). Arrows indicate GFP/SOX9+ or GFP/SOX9/MASH1+ cells. (Scale bar, 100 μm and Scale bar, 30 μm in higher magnification.) (*D*) Example images of MG-derived neurons after ASCL1-ATOH1 expression. HES1 (blue), GFP (green), OTX2 (magenta), and DAPI (gray). Arrowheads show colabeled GFP/HES1/OTX2+ or GFP/HES1/HuC/D+ cells. (Scale bar, 100 μm and Scale bar, 30 μm in higher magnification.) (*E*) Example images of MG-derived OTX2+ neurons after NEUROD1-ASCL1 expression. GFP (green), OTX2 (magenta), MASH1 (ASCL1, red), and DAPI (gray). Arrowheads indicate GFP+ cell colabeled with MASH1 and OTX2. (Scale bar, 100 μm and Scale bar, 30 μm in higher magnification.)

of ASCL1 and NEUROD1 increases the rate of reprogramming from 20% with ASCL1 alone, to over 60%. The increase in reprogramming efficiency further enables the reprogramming of adult postmortem retinal MG; with ASCL1 alone we did not observe neurogenesis in adult retina, but with the combination of ASCL1 with either ATOH1 or NEUROD1, we found some examples of MG-derived neurons of either bipolar and rare examples of HuC/D+ cells (amacrine/RGC fate).

We have also found in mice that different combinations of reprogramming factors direct the progeny of MG to specific retinal cell fates: Overexpression of *Ascl1* induces MG to generate primarily bipolar cells, while most MG-derived neurons expressed HuC/D after overexpression of *Ascl1* and *Atoh1* (5). Although we find similar results with the human MG, there are some differences. For example, while nearly 80% of the neurons generated from MG overexpressing *Ascl1* and *Atoh1* resemble ganglion cells

in mice (8), a similar combination of TFs in the human retina resulted in fewer than 20% of the MG-derived neurons expressing HuC/D. It is not clear why human and mouse MG would behave differently with the same combination of TFs and the identical delivery system. One parsimonious explanation is that 1) the OTX2+ bipolar neurons are generated from MG where the ASCL1 dominates the reprogramming, and this declines with age, like in the mouse and 2) the HuC/D + neurons are generated from MG where the ATOH1 dominates and this does not decline with age, similar to the mouse. However, this discrepancy between species highlights the importance of testing combinations of already known TFs in a human model, as well as exploring additional TFs to potentially unlock still inaccessible cell fates. Future studies will be needed to determine whether these new cells mature and integrate to the existing circuit. In that regard, retinospheres may not be the ideal models to study long-term MG-derived RGC-like cells, as RGCs degenerate over time in this model (32).

Nonetheless, an important advance in our findings is that combining TFs along with ASCL1 can reprogram MG in the adult human retina without the addition of epigenetic modulators. This represents a proof of concept that we can stimulate neurogenesis from human MG using a viral vector. For future clinical applications, it will probably be necessary to opt for a nonintegrative viral vector strategy such as AAVs (adeno-associated virus), though it will be important to control for the fact that the specificity of the glial promoter GFAP, when delivered via an AAV vector, changes over time when used to express proneural TFs (23–25).

Overall, this study constitutes a critical step that will advance in vivo MG reprogramming as a regenerative approach for the retina. Although many barriers still need to be overcome, the fact that neurogenesis can be stimulated in adult human MG shows that this approach may someday lead to a therapeutic strategy to treat patients suffering from retinal diseases.

Materials and Methods

Retinospheres Culture. Human retinal tissues were provided from the Birth Defect Research Laboratory at the University of Washington following the approved protocol (UW5R24HD000836). Retinospheres were cultured as previously debrided (18, 32). Briefly, retinospheres are maintained in low binding attachment plate in Retinal Differentiation Medium (RDM 5%; supplemented with 5% fetal bovine serum (FBS), DMEM/DMEM/F12, 2% B27, 1% Pen-Strep) at 37 °C incubator with 5% CO_2. Age of the retinosphere is defined by the gestational age of the sample at the time of procurement plus the time in vitro culture. For instance, D132+ 77 refers to a sample of 132 d at the time of the procurement that was cultured for an additional 77 d in culture (*SI Appendix*, Table S1). For each experiment of this study, age corresponds to the total age of the retinosphere at the beginning of the experiment (Day 0). Information about samples is listed in *SI Appendix*, Table S1.

Postmortem Human and Mouse Retinal Explants Culture. Deidentified cadaveric posterior eye sections were obtained from Sierra Donor Services Eye Bank (West Sacramento, CA) for this study (*SI Appendix*, Table S2). These were research-grade tissues deemed unsuitable for transplantation, with consent obtained for their use in research in accordance with the Uniform Anatomical Gift Act, Ca. Health and Saf. Code § 7150, Eye Bank Association of America Medical Standards, and Sierra Donor Services Eye Bank Standard Operating Procedures. The peripheral retina, excluding the macula, was meticulously dissected and washed in HBSS containing antibiotics and then carefully segmented for retinal explant culture. Retinal segments approximately 3 mm square were placed with the photoreceptor side facing up onto a 0.4 μm pore culture insert in a 6-well plate. Medium (neural basal medium containing 10% FBS, 1% N2, 1% B27, 0.5% L-glutamine, and 1% Pen-Strep) was changed every other day. Similarly, the same protocol was followed for P12 or adult mouse retinal explants. Virus (*SI Appendix*, Table S3) was pipetted directly onto the surface of the explant. Retinal explants were maintained in culture in incubator at 37 °C with 5% CO_2.

Vector Transduction in 3D Retinospheres. Retinospheres of desired ages were collected and dissected in half. Each retinospheres was then placed in an individual well of a normal attachment 96-well plate. For each condition, individual retinosphere received the same master mix containing RDM5%, Neuraminidase (MilliporeSigma), Polybrene, DMSO, EdU, and the virus (*SI Appendix*, Table S3). The following day, retinospheres were transferred to an individual well of a low binding attachment plate without removing the medium. The next day the medium was replaced with fresh RDM5% and EdU. Viral vectors were sources from VectorBuilder (*SI Appendix*, Table S3).

Tissue Preservation and IHC. Tissue preservation and immunostaining were performed as previously described (18). Briefly, Retinal Tissues (Retinospheres and retinal explants) were fixed with PFA 4% for 15 min prior to embedding in successive solutions containing 10%, 20%, or 30% sucrose for 30 mins each at RT. Tissues were then frozen in OCT and cryosectioned at 15 μm for retinospheres and 18 μm for retinal explants (mouse and human). For immunostaining, sections were washed three times in PBS and then incubated with a blocking solution (10% horse serum, 90% PBS, and 0.5% Triton X-100) for 1 h at RT. Primary antibodies (*SI Appendix*, Table S4) were diluted in the blocking solution and incubated overnight at 4 °C. The following day, sections were washed three times with PBS prior to a 1 h treatment at RT with secondary antibodies (*SI Appendix*, Table S4) primarily diluted in blocking solution containing 1/8,000 DAPI. After three PBS washes, sections were coverslipped using Fluoromount-G (SouthernBiotech) mounting medium. For EdU labeling, the Click-it solution (Click-iT EdU Assay, Invitrogen) was used following the manufacturer's instructions.

Microscopy/Cell Counts and Statistical Analysis. Imaging was performed using a Zeiss LSM880 confocal microscope. For quantification analysis with cell type–specific markers (OTX2, HuC/D, SOX9, HES1), a total of 50 GFP+ cells per retinospheres were included from random sections. GFP/Marker+ cells were then counted with a 20X or 63X objective. Each dot/shape on the bar graph represents an individual retinosphere. Graphics and statistical analysis were performed using GraphPad Prism (version 10.2.2). Welch's *t* test was used for analysis between two conditions. Results are presented as mean ± SD, except Fig. 5*G*, results are presented as mean ± SEM.

Electrophysiology. We recorded electrical responses of transfected GFP+ cells using whole-cell patch clamp techniques. Fluorescent cells were identified using a two-photon microscope, and GFP expression in all recorded cells was confirmed by filling the cells with a second dye (Alexa 594) during recording and checking colocalization with GFP. Patch pipettes were filled with an internal solution containing 123 mM K-aspartate, 10 mM KCl, 10 mM HEPES, 1 mM $MgCl_2$, 1 mM $CaCl_2$, 2 mM EGTA, 4 mM Mg-ATP, 0.5 mM Tris-GTP, and 100 μM Alexa Fluor 594-hydrazide. Whole cell patch pipettes had resistances of 12 to 14 MΩ. Access resistance was < 25 MΩ for all cells. Reported voltages have not been corrected for a ~−10 mV liquid junction potential.

Fluorescent Activated Cell Sorting (FACS). Retinospheres were dissociated into single cells as previously described (18). Following dissociation cells were passed through a 35 μm strainer. FACS was performed to isolate the GFP+ cells using a BD FACSAria III cell sorter (BD Bioscience).

Single-Cell RNA Library Construction. Following FACS purification, GFP+ cells were centrifuged at 300 g at 4 °C for 5 mins. For each sample, cells were resuspended in RDM5% to reach a concentration of 1,000 cells per μl. Libraries construction was done using the Chromium Next GEM single-Cell 3′ Reagent kits v3.1 (Dual Index) following the manufacturer's instructions. Libraries were next sequenced using Illumina NextSeq.

Data, Materials, and Software Availability. Single cell sequencing data have been deposited in GEO/SRA (GSE284180) (34).

ACKNOWLEDGMENTS. We would like to thank Dr. Ian Glass and the members of the BDRL (Birth Defect Research Laboratory) for their valuable help with the human fetal tissues. Thank you to all the members of the Reh lab (past and present) and the Bermingham-McDonogh lab for their valuable comments on the manuscript. This work is funded by a grant from the Foundation Fighting Blindness (TA-RM-0620-0788-UWA) to T.A.R. and by a sponsored research agreement with Tenpoint Therapeutics.

1. J. R. Soucy *et al.*, Retinal ganglion cell repopulation for vision restoration in optic neuropathy: A roadmap from the RReSTORe Consortium. *Mol. Neurodegener* **18**, 64 (2023), https://molecularneurodegeneration.biomedcentral.com/articles/10.1186/s13024-023-00655-y.
2. J. Ribeiro *et al.*, Restoration of visual function in advanced disease after transplantation of purified human pluripotent stem cell–derived cone photoreceptors. *Cell Rep.* **35**, 109022 (2021), 10.1016/j.celrep.2021.109022.
3. A. Salman, M. E. McClements, R. E. Maclaren, Insights on the regeneration potential of müller glia in the mammalian retina. *Cells* **10**, 1957 (2021).
4. J. Pollak *et al.*, ASCL1 reprograms mouse Müller glia into neurogenic retinal progenitors. *Development* **140**, 2619–2631 (2013).
5. Y. Ueki *et al.*, Transgenic expression of the proneural transcription factor Ascl1 in Müller glia stimulates retinal regeneration in young mice. *Proc. Natl. Acad. Sci. U.S.A.* **112**, 13717–13722 (2015).
6. N. L. Jorstad *et al.*, Stimulation of functional neuronal regeneration from Müller glia in adult mice. *Nature* **548**, 103–107 (2017).
7. L. Todd *et al.*, Reprogramming Müller glia to regenerate ganglion-like cells in adult mouse retina with developmental transcription factors. *Sci. Adv.* **8**, eabq7219 (2022), https://www.science.org.
8. L. Todd *et al.*, Efficient stimulation of retinal regeneration from Müller glia in adult mice using combinations of proneural bHLH transcription factors. *Cell Rep.* **37**, 109857 (2021), 10.1016/j.celrep.2021.109857.
9. T. Hoang *et al.*, Gene regulatory networks controlling vertebrate retinal regeneration. *Science* **370**, eabb8598 (2020).
10. N. Le *et al.*, Robust reprogramming of glia into neurons by inhibition of Notch signaling and nuclear factor I (NFI) factors in adult mammalian retina. *Sci. Adv.* **10**, eadn2091 (2024), https://www.science.org/doi/10.1126/sciadv.adn2091.
11. D. Goldman, Müller glial cell reprogramming and retina regeneration. *Nat Rev Neurosci* **15**, 431–442 (2014).
12. M. Lahne, M. Nagashima, D. R. Hyde, P. F. Hitchcock, Reprogramming Müller Glia to regenerate retinal neurons. *Annu. Rev. Vis. Sci.* **6**, 171–193 (2020), 10.1146/annurev-vision-121219-.
13. L. Todd, T. A. Reh, Comparative biology of vertebrate retinal regeneration: Restoration of vision through cellular reprogramming. *Cold Spring Harb. Perspect. Biol.* **14**, a040816 (2022).
14. B. V. Fausett, J. D. Gumerson, D. Goldman, The proneural basic helix–loop–helix gene Ascl1a is required for retina regeneration. *J. Neurosci.* **28**, 1109–1117 (2008).
15. S. G. Wohl, M. J. Hooper, T. A. Reh, MicroRNAs miR-25, let-7 and miR-124 regulate the neurogenic potential of Müller glia in mice. *Development* **146**, dev179556 (2019).
16. N. L. Jorstad *et al.*, STAT signaling modifies Ascl1 chromatin binding and limits neural regeneration from Muller Glia in adult mouse Retina. *Cell Rep.* **30**, 2195–2208.e5 (2020), 10.1016/j.celrep.2020.01.075.
17. L. Todd, C. Finkbeiner, C. K. Wong, M. J. Hooper, T. A. Reh, Microglia suppress Ascl1-induced retinal regeneration in mice. *Cell Rep.* **33**, 108507 (2020), 10.1016/j.celrep.2020.108507.
18. J. Wohlschlegel *et al.*, ASCL1 induces neurogenesis in human Müller glia. *Stem Cell Rep.* **18**, 2400–2417 (2023).
19. T. Furukawa, S. Mukherjee, Z. Z. Bao, E. M. Morrow, C. L. Cepko, Rax, Hes1, and notch1 promote the formation of Muller Glia by postnatal retinal progenitor cells. *Neuron.* **26**, 383–394 (2000).
20. K. Ueno *et al.*, Analysis of Müller glia specific genes and their histone modification using Hes1-promoter driven EGFP expressing mouse. *Sci. Rep.* **7**, 3578 (2017).
21. N. Le, H. Appel, N. Pannullo, T. Hoang, S. Blackshaw, Ectopic insert–dependent neuronal expression of GFAP promoter-driven AAV constructs in adult mouse retina. *Front Cell Dev. Biol.* **10**, 914386 (2022).
22. Y. Xie, J. Zhou, L. L. Wang, C. L. Zhang, B. Chen, New AAV tools fail to detect Neurod1-mediated neuronal conversion of Müller glia and astrocytes in vivo. *EBioMedicine* **90**, 104531 (2023), www.thelancet.com.
23. L. L. Wang *et al.*, Revisiting astrocyte to neuron conversion with lineage tracing in vivo. *Cell* **184**, 5465–5481.e16 (2021).
24. L. S. VandenBosch *et al.*, Developmental changes in the accessible chromatin, transcriptome and Ascl1-binding correlate with the loss in Müller Glial regenerative potential. *Sci. Rep.* **10**, 1–18, (2020), 10.1038/s41598-020-70334-1.
25. A. S. Berrebi *et al.*, Cerebellar Purkinje cell markers are expressed in retinal bipolar neurons. *J. Comp. Neurol.* **308**, 630–649 (1991).
26. Y. Xu *et al.*, Retinal ON bipolar cells express a new PCP2 splice variant that accelerates the light response. *J. Neurosci.* **28**, 8873–8884 (2008).
27. S. H. Chew, C. Martinez, K. R. Chirco, S. Kandoi, D. A. Lamba, Timed notch inhibition drives photoreceptor fate specification in human retinal organoids. *Invest. Ophthalmol. Vis Sci* **63**, 12 (2022).
28. M. L. Kaufman *et al.*, Transcriptional profiling of murine retinas undergoing semi-synchronous cone photoreceptor differentiation. *Dev. Biol.* **453**, 155–167, (2019), 10.1016/j.ydbio.2019.05.016.
29. B. R. Nelson, B. H. Hartman, S. A. Georgi, M. S. Lan, T. A. Reh, Transient inactivation of Notch signaling synchronizes differentiation of neural progenitor cells. *Dev. Biol.* **304**, 479–498 (2007).
30. C. Finkbeiner *et al.*, Single-cell ATAC-seq of fetal human retina and stem-cell-derived retinal organoids shows changing chromatin landscapes during cell fate acquisition. *Cell Rep.* **38**, 110294 (2022).
31. N. Le *et al.*, Robust reprogramming of glia into neurons by inhibition of Notch signaling and nuclear factor I (NFI) factors in adult mammalian retina. *Sci. Adv.* **10**, eadn2091 (2024), https://www.science.org/doi/10.1126/sciadv.adn2091.
32. A. Sridhar *et al.*, Single-cell transcriptomic comparison of human fetal retina, hPSC-derived retinal organoids, and long-term retinal cultures. *Cell Rep.* **30**, 1644–1659.e4 (2020), 10.1016/j.celrep.2020.01.007.
33. K. C. Eldred, T. A. Reh, Human retinal model systems: Strengths, weaknesses, and future directions. *Dev. Biol.* **480**, 114–122, (2021), 10.1016/j.ydbio.2021.09.001.
34. J. Wohlschlegel *et al.*, Stimulating the regenerative capacity of the human retina with proneural transcription factors in 3D cultures. Gene Expression Omnibus (GEO). https://www.ncbi.xyz/geo/query/acc.cgi?acc=GSE284180. Deposited 12 December 2024.